New Materials, Compounds and Applications
Vol.8, No.1, 2024, pp.109-120
https://doi.org/10.62476/nmca8109

STUDY OF CATALYTIC BEHAVIOURS OF THE SPINEL STRUCTURE $Nd_xMg_{1-x}Al_2O_4$ COMPOSITION WITH ZSM-5 ZEOLITE IN ETHYLBENZENE DISPROPORTIONATION

N.I. Mahmudova[1], S.E. Mammadov[1*], A.Z. Mamedova[2], N.F. Akhmedova[1], T.M. Ilyasli[1]

[1]Baku State University, Baku, Azerbaijan
[2]Azerbaijan State Oil and Industry University, Baku, Azerbaijan

Abstract. Nanosized (10–15 nm) powders of spinel structures $Nd_xMg_{1-x}Al_2O_4$ were obtained by low-temperature combustion of aluminium, magnesium, neodymium nitrate solutions, diethylmalonate, and hydrazine monohydrate with further calcination of nanopowders at 1000 °C, which were used in the preparation of catalytic compositions with ZSM-5 zeolite. The obtained catalytic compositions were characterized by X-ray diffraction, pyridine adsorption, and low-temperature nitrogen adsorption. The acidic properties and porosity of the catalysts were altered by controlling the concentration of nanopowder (1.0–7.0 wt.%) in the catalytic composition.
The interaction of the modifier with HZSM-5 zeolite leads to a decrease in specific surface area and pore volume, as well as reduse of strong Bronsted acid sites (B) and an increase in the concentration of medium Lewis acid sites (L), resulting in a change in the B/L ratio from 3.61 to 0.23. The ongoing variations contributed mainly to an enhancement of the para-selectivity of the catalytic composition in the ethylbenzene disproportionation reaction. The catalytic composition of 5% $Nd_{0.1}Mg_{0.9}Al_2O_4$ with a pore volume of 0.15 cm^3/g and an acid site B/L ratio of 0.27 demonstrates a maximum selectivity to p-diethylbenzene of 75.6% with a conversion of ethylbenzene of 23.7%.

Keywords: *Nanosized powders of spinel structures, modification, ZSM-5, neodymium, disproportionation, ethylbenzene.*

Corresponding Author: *Sabit Mammadov, Baku State University, Z. Khalilov 23, Baku, Azerbaijan, Tel.:+994505627065, e-mail: sabitmamedov51@mail.ru*

Received: *27 December 2023;* ***Accepted:*** *19 March 2024;* ***Published:*** *15 April 2024.*

1. Introduction

Para-substituted alkylaromatic hydrocarbons have a wide range of applications in petrochemical and organic synthesis (Sotelo *et al.*, 2010; Tsai *et al.*, 1999; Tsai *et al.*, 2007).

One of the important industrial methods of p-diethylbenzene (p-DEB) production is disproportionation of ethylbenzene (EB) on zeolite catalysts (Tsai *et al., 2007;* Roji *et al.*, 2000; Al-Khattaf *et al.*, 2009; Wang *et al.*, 1993; Janardhan *et al.*, 2014). Zeolite catalysts are now successfully replacing traditional Friedel-Crafts catalysts because of their advantages, such as stability, recyclability, and sustainability.

How to cite (APA):
Mahmudova, N.I., Mammadov, S.E., Mamedova, A.Z., Akhmedova, N.F. & Ilyasli, T.M. (2024). Study of catalytic behaviours of the spinel structure $Nd_xMg_{1-x}Al_2O_4$ composition with zsm-5 zeolite in ethylbenzene disproportionation. *New Materials, Compounds and Applications*, *8*(1), 109-120 https://doi.org/10.62476/nmca8109

The Texture of a zeolite, the type of acid sites, and the reaction medium significantly influence the activity and selectivity of disproportionation reactions of toluene and diethylbenzene, which result in the formation of dialkylbenzenes, including the distribution of para-, m-, and o-isomers (Cejka *et al.,* 2002; Suganuma *et al.*, 2017; Albahar *et al.,* 2020; Mamedov *et al.,* 2009; Raj *et al.,* 2007; Zilkova *et al.,* 2009). The majority of the papers on disproportionation, transalkylation of toluene, and C_8 aromatic hydrocarbons are devoted to studying the effects of acid sites, reaction mechanisms, and the type of zeolite catalysts. Disproportionation and transalkylation reactions were found to be closely related to the Brønsted acid sites. These reactions proceed at the strong acid sites on the outer and inner surfaces of the zeolite (Cejka *et al.,* 2002*;* Suganuma *et al.*, 2017; Zilkova *et al.*, 2009). The disproportion of ethylbenzene (EB) on large-pore zeolites like mordenite and Y usually proceeds through diphenylethane intermediates, and the reaction occurs by a bimolecular mechanism. All DEB isomers can readily diffuse through zeolite channels. Therefore, in the equilibrium mixture of DEB, the p-DEB content is close to the thermodynamic value (~ 24%) (Tsai *et al.,* 1999; Albahar *et al.,* 2020; Mokoena *et al.,* 2018).

Interconnected channels of 10-membered rings with sizes of 0.51 × 0.55 nm and 0.53 × 0.56 nm prevent the formation of a bulky intermediate product on the medium-pore HZSM-5 zeolite, and the disproportionation of EB occurs by the monomolecular mechanism (Albahar *et al.,* 2020; Chen *et al.,* 1996*;*Chen *et al.,* 2002). Isomers of DEB formed in internal pores (0.636 nm) on zeolite type ZSM-5 appear in thermodynamic equilibrium. However, in contrast to p-DEB, it makes steric hindrance for bulky molecules of m- and o-isomers of DEB to diffuse out of zeolite channels (Velasco *et al.,* 1998; Al-Khattaf *et al.,* 2014; Corma *et al.,* 2000). Therefore, the content of p-DEB in the reaction products exceeds the thermodynamic equilibrium value on large-pore zeolites during disproportionation of EB. Hence, in order to enhance p-DEB selectivity, it is indispensable to passivate strong acid sites on the zeolite surface and reduce their pore size by chemical modification (Suganuma *et al.,* 2017; Mamedov *et al.,* 2009; Zhu *et al.,* 2006; Mitsuyoshi *et al.,* 2017).

One common method of modifying zeolites is impregnation with solutions of transition and rare earth metals. Modification of HZSM-5 zeolite with rare-earth metals (Pr, Gd, Ho, and Yb) increased the p-DEB selectivity to 66.5% (Mahmudov *et al.*, 2022). Nevertheless, obtaining catalytic systems by impregnation of the corresponding salts with subsequent oxidation treatment does not usually result in the formation of highly dispersed phases.

In this respect, it is more preferable to obtain nanostructured catalytic systems using nanopowders of the corresponding metals, their oxides, or mixed oxides with high-silica zeolite of the ZSM-5 type.

Catalytic compositions based on lanthanide-magnesium-aluminium spinel nanoparticles with HZSM-5 zeolite showed high activity in the conversion of methanol to C_2–C_4 alkenes and aromatic hydrocarbons (Mahmudova *et al.,* 2022), as well as in toluene disproportionation (Kerimli *et al.,* 2021). The aim of the current paper is to prepare catalytic compositions based on nanopowders of spinel structure $Nd_xMg_{1-x}Al_2O_4$ with high silica zeolite HZSM-5 and study their catalytic behaviour in ethylbenzene disproportionation.

2. Experimental part

2.1. Catalyst preparation

Nd_2O_3, $MgAl_2O_4$, and $Nd_xMg_{1-x}Al_2O_4$ spinel-type samples were obtained by low-temperature combustion (Mahmudova *et al.*, 2022; Kerimli *et al.*, 2021). Amorphous powders were obtained by heating solution of nitrates in water with an alcoholic solution of malonic acid hydrazine. When heated, the following reactions occur when heated:

$$2Mg(NO_3)_2\cdot 6H_2O + 4Al(NO_3)_3\cdot 9H_2O + 5C_3H_8N_4O_2 \xrightarrow{300\,^{\circ}C} 2MgAl_2O_4 + 68H_2O + 15CO_2 + 18N_2$$

$$2(1-2x)Mg(NO_3)_2\cdot 6H_2O + 4Al(NO_3)_3\cdot 9H_2O + 2xNd(NO_3)_3\cdot 6H_2O + Nd(5 + 5x/8)C_3H_8N_4O_2 \xrightarrow{300\,^{\circ}C} 2Nd_xMg_{1-2x}Al_2O_4 + (68+5x/2)H_2O + (15+15x/8)CO_2 + (18+9x/4)N_2$$

We have synthesized nanopowders of the composition $Nd_xMg_{1-x}Al_2O_4$, (where x = 0.05; 0.10, and spinel $MgAl_2O_4$). Nanosized powders (10–15 nm) were obtained by high-temperature treatment of $Nd_xMg_{1-x}Al_2O_4$ nanopowder at 800 °C and 1000 °C. High-silica zeolite ZSM-5 with a molar ratio of 33 (SiO_2/Al_2O_3 = 33) was used as zeolite, which was converted into NH_4-form by ion exchange. The H-form of zeolite was obtained by thermal decomposition of the NH_4-form at 500 °C for 4 hours (Mahmudova *et al.*, 2022). The catalytic compositions were prepared by dry mixing H-form zeolites with nanopowders in an oscillating grinding machine, followed by pressing and calcination in a muffle furnace at 550 °C for 4 hours. The nanopowder content in the catalytic composition was 1.0–7.0 wt.%.

2.2. Characterization

The protonic parent HZSM-5 zeolite was obtained by ion-exchange ZSM-5 with NH_4NO_3 and following calcinations according to the method described (Mamedov *et al.*, 2020).

The catalytic compositions were prepared by dry mixing HZSM-5 zeolites with nanopowders in an oscillating grinder, followed by pressing and calcining in an air current at 350 °C and 550 °C for 4 hours, respectively. The nanopowder content in the catalytic composition was 1.0–7.0 wt.%. The infrared spectra (4000–400 cm^{-1}) were recorded on a BİO-RAD FTS 3000 MX instrument in KBr pellets. IR spectra (4000–400 cm^{-1}) of adsorbed pyridine on modified zeolites were obtained on the BIO-RADFTS 3000MX device using the method described in (Zilkova *et al.*, 2009; Gong et al., 2012; Kazansky *et al.*, 2000). The XRD patterns of the catalytic compositions were collected on a RIGAKU MINIFLEX diffractometer with Cu-Kα radiation (α = 0.15042 nm^{-1}) operated at 40 kV and 30 mA. The catalysts were imaged in a 2θ scanning range from 10° to 80° in 0.0167° scanning increments.

The BET surface area and pore volume of the catalytic composition samples were determined by liquid nitrogen adsorption at 77 K using the Micromeritics ASAP-2010 instrument. The sample (ca. 220 mg) was degassed at 300 °C and 1×10^{-3} Pa for 4 hours before the measurement of data.

2.3. Ethylbenzene conversion

The catalytic ethylbenzene conversion was studied in a flow type fixed-bed reactor (10 cm length, 1.0 cm inner diameter) under atmospheric pressure, packed with 2.0 g of catalyst particles in the isothermal zone of the reactor. The reaction was carried out at temperatures of 300, 350 and 400 °C, space velocity (WHSV) of 1 h-1, with a molar ratio of hydrogen to ethylbenzene equal to 3 and duration of the reaction 3 hours. Before performing the experiments, the catalysts were activated in a stream of air at 500 °C for 2 hours and then maintained at 400 °C for an hour in a hydrogen flow. Various products together with unreacted reagents were condensed in a condenser, and the collected liquid samples were analyzed in a gas chromatograph Agilent GC7890A (Mahmudova *et al.*, 2022).

3. Results and discussion

XRD patterns of the obtained samples thermally treated at 1000 °C are shown in Figure 1.

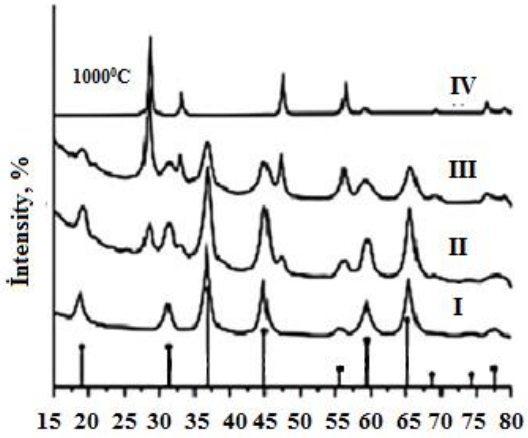

Figure 1. Diffractogram Nd_2O_3 (I), $MgAl_2O_4$ (II), $Nd_{0,05}Mg_{0,05}Al_2O_4$ (III), $Nd_{0,1}Mg_{0,9}Al_2O_4$ (IV) dependence of the particle size on the annealing temperature

As can be seen, the intensity of X-ray diffraction of the spinel phase grows with increasing annealing temperature, and simultaneously, the width of the reflection narrows. Perfect crystals are obtained at an annealing temperature of 1000 °C. Neodymium substitutes Mg^{2+} cations and holds cationic positions in the spinel structure. The particle size of the obtained nanopowders is 10-15 nm.

The XRD patterns (Fig. 2**)** of the HZSM-5 and modified catalysts demonstrate that the entire zeolite structure remains almost undisturbed after modification.

Thus, the diffraction peaks of the catalytic compositions correspond to those of HZSM-5 (2θ = 7.8°, 8.7°, 23.0°, 23.8°, 24.2°) (Gong *et al.*, 2012; Tian *et al.*, 2021; Li *et al.* 2021). Comparing with the starting zeolite HZSM-5, new peaks appear in the modified catalysts at 2θ = 23.2° and 23.6°, and the peak at 24.2° is considerably reduced. The intensity of the peak at 23.6° rises with increasing amounts of the modifier, possibly due to its interaction with the HZSM-5 texture (Gong *et al.*, 2012; Li *et al.*, 2018). It is evident that the modifiers are well dispersed on the zeolite surface.

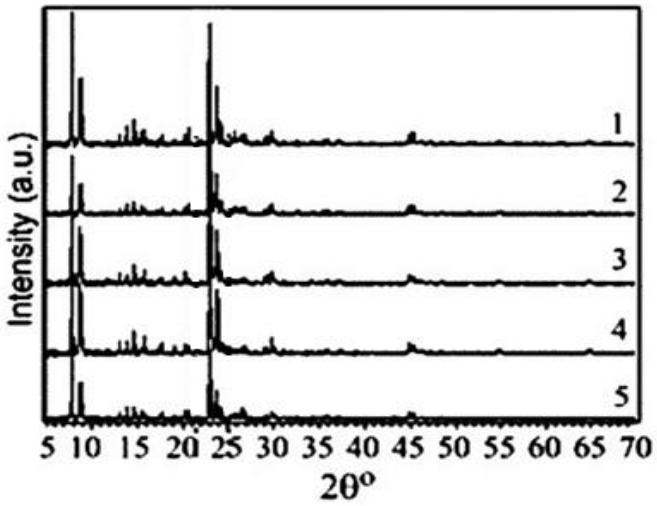

Figure 2. XRD patterns of catalysts: 1) HZSM-5, 2) 1%$Nd_{0.1}Mg_{0.9}Al_2O_4$/HZSM-5, 3) 3%$Nd_{0.1}Mg_{0.9}Al_2O_4$/HZSM-5, 4) 5%$Nd_{0.1}Mg_{0.9}Al_2O_4$/HZSM-5, 5) 7%$Nd_{0.1}Mg_{0.9}Al_2O_4$/ HZSM-5

IR spectra in the (400–1400) cm^{-1} region (Fig. 3) confirm the conclusion about the preservation of the HZSM-5 texture during further treatment with Nd salts.

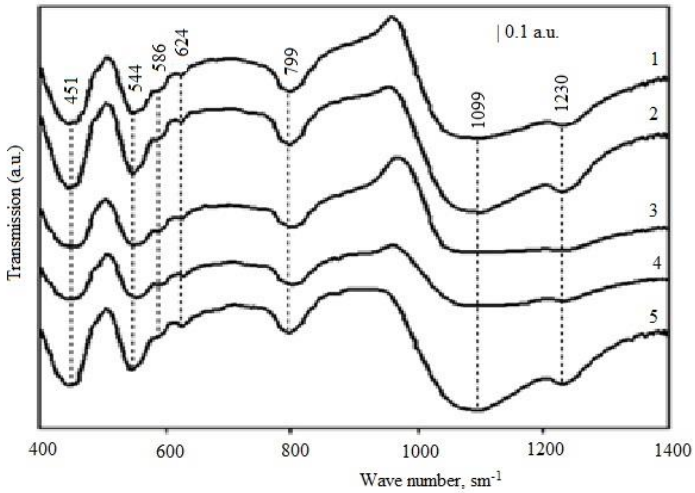

Figure 3. Infrared spectra of HZSM-5 (1), 1%$Nd_{0.1}Mg_{0.9}Al_2O_4$/HZSM-5, (3) 3% $Nd_{0.1}Mg_{0.9}Al_2O_4$/HZSM-5, (4) 5%$Nd_{0.1}Mg_{0.9}Al_2O_4$/HZSM-5, (5) 7% $Nd_{0.1}Mg_{0.9}Al_2O_4$/HZSM-5

Thus, impregnation does not affect the bands characteristic of Si-O-Si and Si-O-Al fragments (Zhu *et al.*, *2006*, Ryczkowski, 2001). Meanwhile, the catalysts contain characteristic IR vibrations of the TO_4 stretching region (799 cm^{-1}) and asymmetric and symmetric vibrations of the TO binding/double rings (624, 586, 544, and 451 cm^{-1}) derived from HZSM-5 (Yoo *et al.*, 2000). In the case of $Nd_xMg_{1-x}Al_2O_4$/HZSM-5, the IR bands corresponding to $Nd_xMg_{1-x}Al_2O_4$-O fragments were not clearly observed, while a slightly noticeable bathochromic shift of TO-binding/double ring bands (624, 544, and 451 cm^{-1}) occurs with a decline in their intensity (Fig. 3).

Table 1. Influence of $Nd_{0.1}Mg_{0.9}Al_2O_4$ nanopowder amount in the catalytic composition (HZSM-5) on the ethylbenzene disproportionation reaction

Amount of modifier, %	T, °C	Conversion, %	Benzene	Gases	m-DEB	p-DEB	o-DEB	Others*
-	300	30.9	11.71	0.03	10.91	7.62	0.31	0.42
	330	36.7	14.0	0.06	12.64	7.86	0.57	1.57
	350	41.4	15.1	0.08	13.63	8.42	1.42	2.75
1,0	300	28.6	10.22	0.04	9.03	8.96	0.14	0.21
	330	34.2	13.1	0.07	10.71	9.22	0.18	0.92
	350	37.8	14.7	0.11	11.76	9.34	0.30	1.75
3,0	300	26.6	9.83	0.05	5.32	10.97	-	0.13
	330	30.6	11.84	0.09	66.61	11.63	-	0.43
	350	35.7	14.58	0.12	8.12	12.34	0.12	0.72
5,0	300	23.7	8.24	0.06	3.82	11.47	-	0.11
	330	27.7	10.88	0.10	4.63	11.86	-	0.23
	350	32.5	14.32	0.13	5.26	12.34	-	0.45
7,0	300	17.6	4.91	0.09	2.96	9.58	-	0.06
	330	20.9	6.78	0.14	3.72	10.12	-	0.14
	350	24.4	8.42	0.23	4.47	10.97	-	0.31

*–Includes toluene, xylenes and trimethylbenzenes

Thus, the modification of HZSM-5 with $MgAl_2O_4$, Nd_2O_3, $Nd_{0.05}Mg_{0.95}Al_2O_4$, and $Nd_{0.1}Mg_{0.9}Al_2O_4$ nanopowders leads to a considerable enhancement of its para-selectivity (PS) in the disproportionation reaction (Fig. 4).

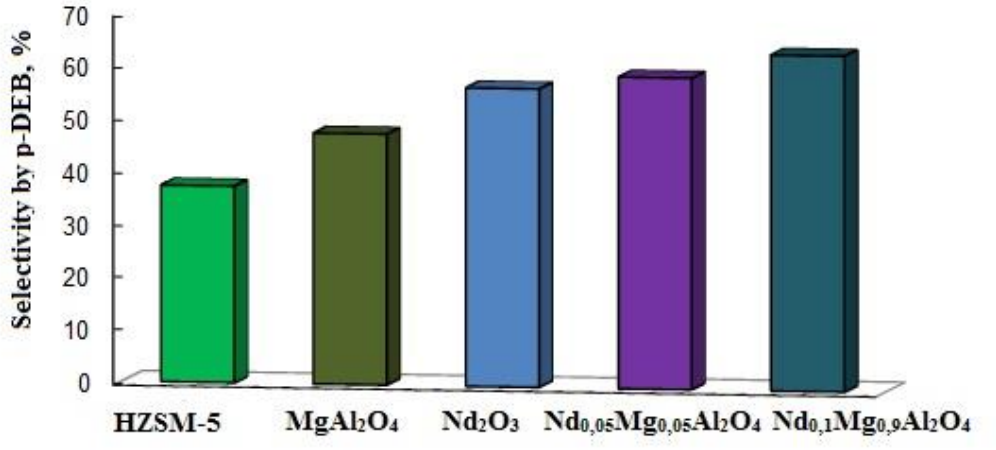

Figure 4. Modifier nanopowders effect on the p-DEB selectivity (para-selectivity*) in the disproportionation reaction of toluene. The content of the modifiers is 3.0 wt.% (T = 330 °C, v = 1 h^{-1}). *Selectivity by p-DEB, % = p-DEB amount in a mixture, (wt.%)/S_{DEB}, (wt. %)

The type of modifier significantly affects its para-selectivity. Moreover, selectivity by p-DEB on unmodified HZSM-5 zeolite at 330 °C is 37.3%. Catalytic compositions of HZSM-5 zeolite with 3.0 wt.% modifier nanopowders display greater selectivity to p-DEB.

The catalyst modified with $MgAl_2O_4$ nanopowders shows the lowest selectivity for p-DEB (47.6%) among the catalytic compositions, and the highest selectivity for p-DEB is demonstrated by the $Nd_{0.1}Mg_{0.9}Al_2O_4$ nanopowders modified ones (63.7%).

The unmodified HZSM-5 zeolite in the entire temperature range under study (300-350 °C) leads to the formation of all three DEB isomers, which is obviously explained by

the isomerization of p-DEB into m- and o-DEB on the strong Brønsted acid sites localized on the outer surface of the zeolite (Table 1). As the reaction temperature rises from 300 °C to 350 °C, the content of o-DEB (from 0.31 to 1.42 wt.%) and m-DEB (from 10.91 to 13.63 wt.%) grows. The m-DEB content in the reaction products is higher than the p-DEB content in the studied temperature intervals (m-DEB/p-DEB=1.43-1.62)

HZSM-5 modification with $Nd_{0.1}Mg_{0.9}Al_2O_4$ nanopowder reduces the conversion of ethylbenzene. However, a decrease in by-product content occurs in this case. The most noticeable decline in ethylbenzene conversion content is observed on catalysts containing 3.0–7.0 wt.% of the modifier.

In comparison with the catalyst modified with 3.0–7.0 wt.% of the modifier, the unmodified sample HZSM-5 does not exhibit o-DEB production in the studied temperature interval. In addition, at 300–350 °C on catalytic compositions with 3.0–7.0 wt.% modifier, the p-DEB content is always higher than the m-DEB content. The highest p-DEB selectivity is achieved at 300 °C. Fig. 5 illustrates the rise in p-DEB selectivity with an increase in the content of the modifier in the catalytic composition.

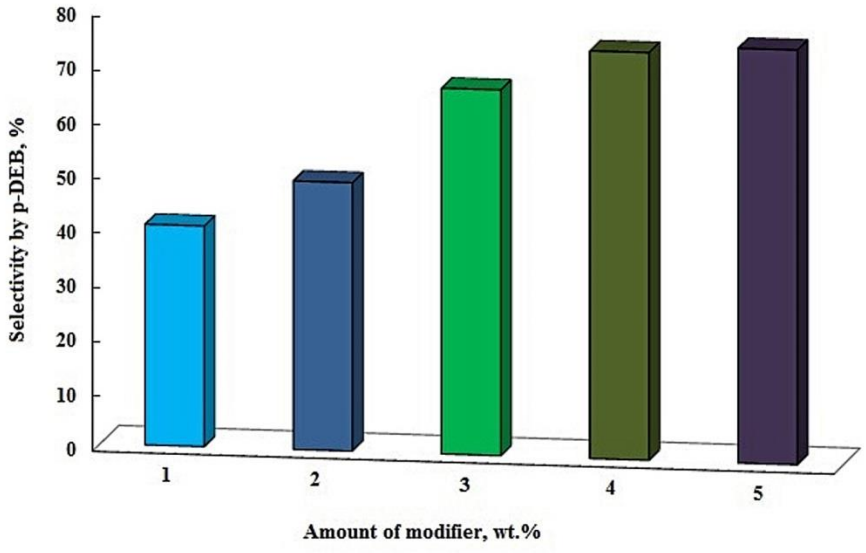

Fig. 5. Relation of p-DEB selectivity and the content of the $Nd_{0.1}Mg_{0.9}Al_2O_4$ modifier

A gradual decline in p-DEB selectivity occurs with temperature growth. The highest p-DEB selectivity at 300–350 °C is displayed by catalysts with 5.0 and 7.0 wt.% modifiers and is 70.1–75.6% and 71.0–75.0%, respectively. However, on the 7.0% $Nd_{0.1}Mg_{0.9}Al_2O_4$/HZSM-5 catalyst, high selectivity to p-DEB is achieved at a low conversion (17.6%) of ethylbenzene. Thus, the most effective catalyst among the investigated compositions can be considered 5% $Nd_{0.1}Mg_{0.9}Al_2O_4$/HZSM-5, where high selectivity by p-DEB is achieved at higher conversion (23.7%) of ethylbenzene.

The high selectivity of catalysts modified with $Nd_{0.1}Mg_{0.9}Al_2O_4$ nanopowders may be due to a change in their acid and texture properties as a result of modification.

The infrared spectra of catalysts degassed at 200 °C and 350 °C are shown in Fig. 6. The IR spectra show absorption bands at 1450, 1490, and 1540 cm^{-1}.

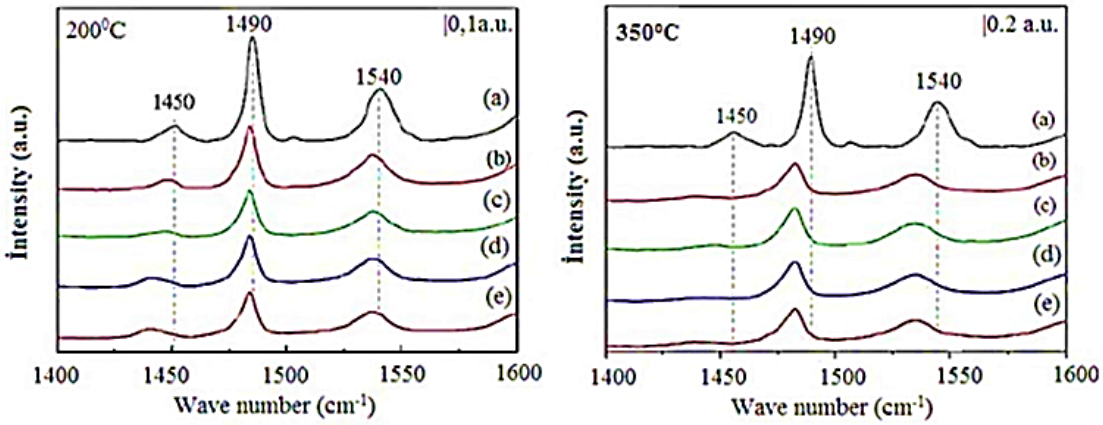

Fiq. 6. Py-IR spectra of catalysts deqassed at 200 °C and 350 °C (a), HZSM-5 (b), 3.0 wt.% $Nd_{0.1}Mg_{0.9}Al_2O_4$ (c); 5.0 wt.% $Nd_{0.1}Mg_{0.9}Al_2O_4$ (d); 7.0 wt.% $Nd_{0.1}Mg_{0.9}Al_2O_4$ (e)

The absorption band at 1450 cm^{-1} should be assigned to the adsorption of pyridine coordinated with Lewis acid sites (L), and the absorption band at 1540 cm^{-1} is due to pyridine ions (Gong *et al.*, 2012; Yoo *et al.*, 2000; Zhang *et al.*, 2009). In addition, the absorption band at 1490 cm^{-1} is associated with vibrations of the pyridine ring at the B- and L-acid sites. The results confirm the existence of B- and L-acid sites on these catalysts. The B- and L-acid sites observed at 200 °C can be classified as weak and moderate acid sites, and the B- and L-acid sites detected at 350 °C can be assigned to the strong acid sites. By increasing the content of the modifier in the catalyst, the IR absorption bands belonging to the B- and L-acid sites shift to the low-frequency region. As the modifier content grows, the concentration of strong B- and L-acid sites decreases.

Table 2 demonstrates as follows: The unmodified HZSM-5 has a higher total concentration of B-acid sites and a lower total concentration of L-acid sites than the modified catalysts. HZSM-5 has the highest B/L ratio of acid sites (3.61).

Table 2. Effect of $Nd_{0.1}Mg_{0.9}Al_2O_4$ nanopowder content in the catalyst composition on the distribution of Brønsted and Lewis acid sites

Amount of $Nd_{0.1}Mg_{0.9}Al_2O_4$ nanopowder	**Concentration B, μmol/g**			**Concentration L, μmol/g**			
	Weak and Medium, 200 °C	**Strong, 350 °C**	**Total**	**Weak and Medium, 200 °C**	**Strong, 350 °C**	**Total**	**B/L**
0	550	370	920	140	115	255	3.61
1	110	230	340	230	90	320	1.06
3	90	180	270	450	80	530	0.51
5	70	150	220	740	70	810	0.27
7	65	140	205	810	60	870	0.23

Unmodified zeolite has a high concentration of weak, medium and strong Brønsted acid sites.

A significant change occurs in the distribution of the Brønsted and Lewis acid sites with increasing the content of the modifier. An increase in the modifier content from 1.0 to 7.0 wt.% leads to a drop in the concentration of weak, medium and strong Brønsted acid sites. This is accompanied by an increase in the concentration of weak Lewis acid sites (from 230 to 810 μmol/g) and a decline in the concentration of strong Lewis acid sites (from 90 μmol/g to 60 μmol/g). The changes in acid site concentrations result in a considerable reduction of the B/L ratio from 3.61 to 0.23. The introduction of the

$Nd_{0.1}Mg_{0.9}Al_2O_4$ modifier into HZSM-5 changes not only the concentration of acid sites, but also affects the distribution of acid sites. Moreover, the loading of the modifier increased the concentration of L-acid sites and decreased the concentration of B-acid sites and the B/L ratio.

Thus, the content of the modifier in the catalyst plays an important role in reducing the concentration and strength of the Brønsted acid sites.

Modifying HZSM-5 zeolite with the modifier $Nd_{0.1}Mg_{0.9}Al_2O_4$ also affects its textural properties (Table 3).

Table 3. Effect of $Nd_{0.1}Mg_{0.9}Al_2O_4$ nanopowder content in the catalyst on its textural behavior

Amount of $Nd_{0.1}Mg_{0.9}Al_2O_4$ nanopowder	**S, m^2/g**	**V_{por}, cm^3/g**
0	263	0.24
1	259	0.23
3	237	0.18
5	221	0.15
7	211	0.13

The loading of 1.0 wt.% of the modifier negligibly affects its specific surface area and the total pore volume of the catalyst. The greatest reduction in specific surface area and pore volume is achieved on catalysts containing 5.0–7.0 wt.% of the modifier. Thus, the specific surface area goes down from 259 to 211–221 cm^2/g, and the total pore volume from 0.24 to 0.13 cm^3/g.

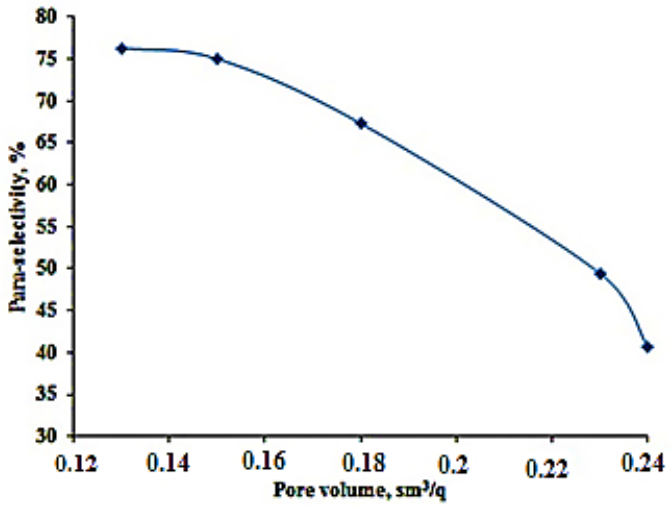

Fig. 7. Relation between para-selectivity and catalyst pore volume at a reaction temperature of 500 °C

Fig. 7 clearly shows that p-DEB selectivity significantly depends on the catalyst pore volume. A reduction of the catalyst pore volume is followed by an enhancement of p-DEB selectivity.

The conversion of the reactant and the selectivity of the reaction yields are well-known to be determined by the pore sizes through which molecules of only certain sizes and shapes pass (Tsai *et al.*, 2010; Cejka *et al.*, 2002; Mitsuyoshi *et al.*, 2017).

Molecules with ≥0.55 nm size can diffuse through the pores of modified ZSM-5 types of zeolites. Diffusion of m- and o-DEB (kinetic diameter ~ 0.68 nm) from pores of

modified zeolite is not feasible. Therefore, p-DEB formed on the acid sites inside the channels can diffuse readily from the zeolite pores. M- and o-DEB can be formed only on the acid sites on the outer surface of zeolite crystals.

Modification of HZSM-5 zeolite with 5.0–7.0 wt.% nanopowder deactivates strong Brønsted acid sites, which leads to a dramatic reduction of m-DEB concentration and avoids o-DEB formation. Thus, the differences in p-DEB selectivity on unmodified and modified catalysts can be explained by a decrease in the total pore volume and the ratio of the number of acid sites (B/L). The catalytic composition containing 5.0 wt. % $Nd_{0.1}Mg_{0.9}Al_2O_4$/HZSM-5 with a pore volume of 0.15 cm^3/g and a B/L ratio of 0.27 represented the highest selectivity of p-DEB (75.6%) at a conversion of EB equal to 23.7%.

4. Conclusion

The loading of $Nd_{0.1}Mg_{0.9}Al_2O_4$ nanopowder into the HZSM-5 zeolite composition leads to a significant change in the textural, acidic, and catalytic behaviors of the catalyst in the ethylbenzene disproportionation reaction.

Selectivity for p-diethylbenzene (DEB) during disproportionation of ethylbenzene in the presence of zeolite composition with $Nd_{0.1}Mg_{0.9}Al_2O_4$ spinel nanopowders is determined by three factors: the modifier concentration, the ratio B/L of acid sites, and the catalyst pore volume.

The maximum selectivity for p-diethylbenzene is obtained in the catalytic composition with 5.0 wt.% $Nd_{0.1}Mg_{0.9}Al_2O_4$ spinel nanopowders and is 75.6%.

References

Albahar, M., Li, C., Zholobenko, V.L., & Garforth, A.A. (2020). The effect of ZSM-5 zeolite crystal size on p-xylene selectivity in toluene disproportionation. *Microporous and Mesoporous Materials,* 302, 110221-11025

Al-Khattaf, S., Ali, S.A., Aitani, A.M., Žilková, N., Kubička, D., & Čejka, J. (2014). Recent advances in reactions of alkylbenzenes over novel zeolites: the effects of zeolite structure and morphology. *Catalysis Reviews*, *56*(4), 333-402.

Al-Khattaf, S., Tukur, N.M., & Rabiu, S. (2009). Ethylbenzene transformation over a ZSM-5-based catalyst in a riser simulator. *Industrial & Engineering Chemistry Research, 48*(6), 2836-2843.

Cejka, J., Wichterlova, B. (2002). Acid-catalyzed synthesis of mono- and dialkyl benzenes over zeolites: active sites, zeolite topology, and reaction mechanisms. *Catalysis Reviews Science and Engineering*, *44*(3), 375-421.

Chen, W.H., Jong, S.J., Pradhan, A., Lee, T.Y., Wang, I., Tsai, T.C., & Liu, S.B. (1996). Coking and Deactivation of H-ZSM-5 Zeolites during Ethylbenzene Disproportionation: I. Formation and Location of Coke. *Journal of the Chinese Chemical Society, 43*(4), 305-313.

Chen, W. H., Tsai, T. C., Jong, S. J., Zhao, Q., Tsai, C. T., Wang, I., ... & Liu, S. B. (2002). Effects of surface modification on coking, deactivation and para-selectivity of H-ZSM-5 zeolites during ethylbenzene disproportionation. *Journal of Molecular Catalysis A: Chemical*, *181*(1-2), 41-55.

Corma, A., Chica, A., Guil, J. M., Llopis, F. J., Mabilon, G., Perdigón-Melón, J. A., & Valencia, S. (2000). Determination of the pore topology of zeolite IM-5 by means of catalytic test reactions and hydrocarbon adsorption measurements. *Journal of Catalysis*, *189*(2), 382-394.

Gong, T., Zhang, X., Bai, T., Zhang, Q., Tao, L., Qi, M., ... & Zhang, L. (2012). Coupling conversion of methanol and C4 hydrocarbon to propylene on La-modified HZSM-5 zeolite catalysts. *Industrial & engineering chemistry research*, *51*(42), 13589-13598.

Janardhan, H.L., Shannbhag, G.V., & Halgeri, A.B. (2014). Shape-selective catalysis by phosphate modified ZSM-5: Generation of new acid sites with pore narrowing. *Applied Catalysis A: General 471*, 12-18.

Kazansky, V.B., Borovkov, V.Y., Serykh, A.I., Santen, R.A., & Anderson, B.G. (2000). Nature of the sites of dissociative adsorption of dihydrogen and light paraffins in ZnHZSM-5 zeolite prepared by incipient wetness impregnation. *Catalysis Letters*, *66*, 39–47.

Kerimli, F. S., Ilyasli, T. M., Mammadov, S. E., Akhmedova, N. F., Mammadov, E. S., Makmudova, N. I., & Akhmedov, E. I. (2021). Evaluation of the Properties of ZSM-5 Type Zeolites Modified with Ce x Mg1–x Al2O4 Nanopowders in the Toluene Disproportionation Reaction. *Petroleum Chemistry*, *61*(8), 895-900.

Li, X., Alwakwak, A.-A., Rezaei, F., & Rownaghi, A.A. (2018). Synthesis of Cr, Cu, Ni, and Y-Doped 3D-Printed ZSM-5 Monoliths and Their Catalytic Performance for n-Hexane Cracking. *ACS Applied Energy Materials, 1*(6), 2740–2748.

Mahmudov, K.T., Kerimli, F.S., Mammadov, E.S., Gurbanov, A.V., Akhmedova, N.F., & Mammadov, S.E. (2022). Catalytic Disproportionation of Ethylbenzene over Ln-Modified HZSM-5 Zeolites. *Petroleum Chemistry*, *62*(8), 933-941.

Mahmudov, K.T., Kerimli, F.S., Mammadov, E. S., Gurbanov, A.V., Akhmedova, N.F., & Mammadov, S.E. (2022). Catalytic Disproportionation of Ethylbenzene over Ln-Modified HZSM-5 Zeolites. *Petroleum Chemistry, 62*(8), 933-941.

Makhmudova, N.I., Ilyasly, T.M., Mammadov, S.E., & Abbasova, R.F. (2022). Synthesis and properties of spinel phases of the composition $Ho_xPr_xMg_{1-2x}Al_2O_4$. *New Materials, Compounds and Applications*, *6*(1), 75-84.

Mamedov, S.E., Akhmedov, E.I., Ismailova, S.B., & Shamilov, N.T. (2009). Effect of phosphorus content on the physicochemical and catalytic properties of pentasils in the ethylbenzene disproportionation reaction. *Petroleum Chemistry, 49*, 133-135.

Mamedov, S.E., Iskenderova, A.A., Akhmedova, N.F., & Mamedov, E.S. (2020). The influence of modification on the properties of high-silica TsVM zeolite in the benzene alkylation reaction with ethanol. *Petroleum Chemistry*, *60*, 950-956.

Mitsuyoshi, D., Kuroiwa, K., Kataoka, Y., Nakagawa, T., & Kosaka, M. (2017). Shape selectivity in toluene disproportionation into para-xylene generated by chemical vapor deposition of tetramethoxysilane on MFI zeolite catalyst. *Microporous and Mesoporous Materials, 242*, 118-126.

Mokoena, K., Scurrell, M.S. (2018). Alkyl transfer reactions on solid acids. The disproportionation of ethylbenzene and toluene on H-mordenite and HY zeolites. *Petroleum Science and Technology*, *36*(16), 1208-1215.

Raj, K.J.A., Meenakshi, M.S., & Vijayaraghavan, V.R. (2007). Ethylation and disproportionation of ethylbenzene over substituted AFI type molecular sieves. *Journal of Molecular Catalysis A: Chemical*, *270*(1–2), 195-200.

Roji, I., Shinobu, Y., Hirohito, O., Hajime, K., & Kazuyoshi, I. (2000). Process for producing aromatic compounds by dealkylation, transalkylation, or disproportionation. *Patent USA US-6040490-A.*

Ryczkowski, J. (2001). IR spectroscopy in catalysis. *Catalysis Today*, *68*, 263-381.

Sotelo, J.L., Rodríguez, A., Águeda, V.I., & Gómez, P. (2010). Supercritical fluids as reaction media in the ethylbenzene disproportionation on ZSM-5. *The Journal of Supercritical Fluids*, *55*(1), 241-245.

Suganuma, S., Nakamura, K., Okuda, A., & Katada, N. (2017). Enhancement of catalytic activity for toluene disproportionation by loading Lewis acidic nickel species on ZSM-5 zeolite. *Molecular catalysis, 435*, 110-117.

Tian, H., Yang, X., Tian, H., Zha, F., Guo, X., & Tang, X. (2021). Realization of rapid synthesis of H-ZSM-5 zeolite by seed-assisted method for aromatization reactions of methanol or methane. *Canadian Journal of Chemistry*, *99*(11), 874-880.

Tsai, T.-C., Liu, S.-B., & Wang, I. (1999). Disproportionation and transalkylation of alkylbenzenes over zeolite catalysts. *Applied Catalysis A: General*, *181*, 355-398.

Tsai, T.-C., Wang, I., Huang, C.-K., & Liu, S.-D. (2007). Supercritical fluids as reaction media in the ethylbenzene disproportionation on ZSM-5. *Applied Catalysis A: General*, *321*(2), 125-134.

Velasco, N. D., Machado, M. D. S., & Cardoso, D. (1998). Ethylbenzene disproportionation on HZSM-5 zeolite: the effect of aluminum content and crystal size on the selectivity for p-diethylbenzene. *Brazilian Journal of Chemical Engineering*, *15*, 184-190.

Wang, I., Tsai, T.C., & Aye, C.L. (1993). Interactions in monoalkylbenzenes disproportionation among zeolite characteristics and reaction mechanisms. *Studies in Surface Science and Catalysis*, *75*, 1673-1676.

Yoo, J., Lee, C., Chang, J., Park, S., & Ko, J. (2000). Characterization and catalytic properties of Ti-ZSM-5 prepared by chemical vapor deposition. *Catalysis Letters*, *66*, 169-173.

Zhang, X., Zhong, J., Wang, J., Zhang, L., Gao, J., & Liu, A. (2009). Catalytic performance and characterization of Ni-doped HZSM-5 catalysts for selective trimerization of n-butene. *Fuel Processing Technology*, *90*, 863-870.

Zhu, Z., Chen, Q., Xie, Z., Yang, W., Kong, D., & Li, C. (2006). Shape-selective disproportionation of ethylbenzene to para-diethylbenzene over ZSM-5 modified by chemical liquid deposition and MgO. *Journal of Molecular Catalysis A: Chemical*, *248*(1-2), 152-158.

Žilková, N., Bejblová, M., Gil, B., Zones, S. I., Burton, A. W., Chen, C. Y., ... & Čejka, J. (2009). The role of the zeolite channel architecture and acidity on the activity and selectivity in aromatic transformations: The effect of zeolite cages in SSZ-35 zeolite. *Journal of Catalysis*, *266*(1), 79-91.